

Supplemental Information

Table of Contents

1) Supplemental Appendix

Summary of prior studies on treatment of myocardial ischemia with VEGF-A

2) Supplemental Tables

Suppl. Table 1. Selected animal studies of cardiac revascularization with VEGF-A

Suppl. Table 2. Selected, placebo-controlled clinical trials of cardiac revascularization with VEGF-A

Suppl. Table 3. Summary of the differences between DNA or modRNA delivery to the heart.

Suppl. Table 4. Open Reading Frame sequences used for modRNA production

Suppl. Table 5. Antibodies used in this study

Suppl. Table 6. Primer sequences

3) Supplemental Methods

4) Supplemental References

5) Supplemental Figures

Suppl. Fig. 1. Efficient modRNA-mediated gene transfer to cardiac and skeletal muscles *in vitro*.

Suppl. Fig. 2. Efficient modRNA-mediated gene transfer to skeletal muscles *in vivo*.

Suppl. Fig. 3. modRNA did not elicit the innate immune response *in vitro* or *in vivo*.

Suppl. Fig. 4. VEGF-A modRNA reduced scar area after MI.

Suppl. Fig. 5. Quantification of MRI data in VEGF-A modRNA and control treated mice.

Suppl. Fig. 6. VEGF-A modRNA upregulated epicardial and endothelial markers in the peri-infarct region after MI.

Suppl. Fig. 7. VEGF-A modRNA upregulated *Wt1* expression in heart tissue but not in remote tissues.

Suppl. Fig. 8. qRT-PCR, FACS analysis, and immunostaining demonstrating the effect of VEGF-A on epicardial cell fate *in vitro*.

Suppl. Fig. 9. VEGF-A modRNA mobilized EPDCs (*Wt1*^{CreERT2} lineage) from the epicardial surface and enhanced their myocardial penetration and differentiation into cardiovascular lineages.

Suppl. Fig. 10. The effect of VEGF-A on gene expression level in adult mouse cardiomyocytes, *in vitro*.

Suppl. Fig. 11. The kinetics of modRNA gel gene transfer to epicardial cells.

Suppl. Fig. 12. VEGF-A modRNA mobilized EPDCs (Cre modRNA gel lineage) from the epicardial surface and enhanced their myocardial penetration and differentiation into cardiovascular lineages.

6) Supplemental Movies

Suppl. Movie 1. Cine MRI of sham-operated heart, 21 days after operation

Suppl. Movie 2. Cine MRI of MI heart, vehicle treated heart, 21 days after operation

Suppl. Movie 3. Cine MRI of MI heart, VEGF-A modRNA treated, 21 days after operation

1. Supplemental Appendix

Summary of Prior Studies on Treatment of Myocardial Ischemia with VEGF-A

Interest in VEGF-A as a therapeutic for ischemic cardiomyopathy was initially driven by its well-established roles in vascular development during embryogenesis⁴⁸ and vascular homeostasis in adult mammals⁴⁹. Tissue ischemia is a potent stimulator of VEGF-A expression, which in turn stimulates neovascularization. Compromised VEGF-A signaling leads to abnormal vasculature in mouse models^{50, 51}. Genetically modified mice that lack several splice isoforms of VEGF-A (VEGF-A₁₆₄ and VEGF-A₁₈₈) exhibit abnormal vasculature and develop ischemic cardiomyopathy in adulthood⁵². VEGF-A levels are elevated after myocardial infarction in animal models and patients; however, the natural history of ischemic cardiomyopathy reveals that endogenous VEGF-A is not sufficient to rescue large areas of myocardium affected by narrowed or blocked coronary arteries^{53, 54}. It was hypothesized, therefore, that delivery of exogenous VEGF-A might lead to therapeutic neovascularization.

Formation of new blood vessels in ischemic myocardium with VEGF-A recombinant protein has been attempted in several animal models (Suppl. Table 5) and in humans (Suppl. Table 4). Neovascularization was consistently observed, but improvement of cardiac function occurred in only a subset of studies. At least one study noted increased vascular permeability and cardiac edema as potential problems with VEGF-A induced neovascularization. Effect on long term survival was not reported in the animal studies. Initial human trials of therapeutic revascularization involving recombinant VEGF-A suggested possible enhancement of vessel formation⁵⁵, but subsequently published placebo-controlled trials did not reveal statistically significant benefit with therapy (Suppl. Table 4).

These studies of VEGF-A in treatment of MI have used several different delivery platforms, each with their own limitations. Recombinant VEGF-A protein was injected into several locations, including the vascular system (intravenous or coronary arterial injections) and the affected myocardium itself. The very short half-life of VEGF-A protein in plasma (estimated to be ~34 minutes in humans) made it difficult to achieve a therapeutically relevant dose⁵². Administration of high doses of recombinant VEGF-A protein was limited by hypotension, thought to be the result of VEGF-A-mediated upregulation of nitric oxide⁵⁶. The very brief “pulse” of protein produced with recombinant VEGF-A did not always result in lasting revascularization. This failure was attributed, in large part, to rapid degradation of recombinant VEGF-A⁵⁷.

In order to increase the total delivered dose of VEGF-A, investigators turned to DNA expression vectors (both viral and non-viral). In several animal models, DNA expression vectors were found to produce higher levels of VEGF-A expression over longer periods of time than could be achieved with recombinant protein. In these studies, VEGF-A-mediated neovascularization was associated with reduction in infarct size as compared with untreated controls⁵⁸⁻⁶¹. In some cases, improved myocardial function was also observed⁵⁹. Adenoviral expression vectors were found to produce higher levels of VEGF-A than the non-viral vectors available at that time. Improved VEGF-A expression with adenoviral vectors led to more robust neovascularization, but came at the cost of untoward effects, including systemic inflammation⁶². In addition, the new vessels were generally immature and leaky, and in some cases produced local edema⁵⁸. Formation of angiomas was also reported⁶³. Most placebo-controlled human trials of cardiac

revascularization therapy with VEGF-A expressed with DNA vectors did not show benefit with therapy (Suppl. Table 5)⁶⁴.

A new generation of non-viral expression vectors has since been used to express high levels of VEGF-A₁₆₅ in vivo without the inflammation associated with adenoviral systems. Such plasmids were reported to reduce infarct size in an ovine model of acute myocardial infarction⁶⁵. In a preliminary human trial of this non-viral plasmid, no untoward effects were observed, but efficacy could not be assessed definitively due to the trial's open-label, non-controlled design⁶⁶. Non-viral, hypoxia-inducible plasmid expression systems for VEGF-A have also been reported. These inducible systems were shown to be effective in rabbit models of acute myocardial infarction, but the results of human testing are not yet available^{61, 67}.

Recently, Lin and coworkers reported the results of delivering a combination of recombinant VEGF-A₁₆₅ protein and self-assembling peptide nanofibers directly to infarcted rat and pig hearts⁶⁸. The nanofibers slowed the degradation of recombinant VEGF-A protein in situ. This observation is consistent with prior studies involving recombinant paracrine factors "loaded" onto nanofibers and then delivered to affected tissues⁶⁹. The "pulse" of VEGF-A expression in situ produced with the nanofiber technique is longer than could be achieved with tolerable doses of recombinant VEGF-A alone, but shorter than the duration of expression with adenoviral vectors⁶⁸. The recombinant VEGF-A-nanofiber combination led to effective revascularization and myocardial tissue remodeling without tissue edema or other untoward effects. Interestingly, the VEGF-A-nanofiber combination recruited new cardiomyocyte-like cells within the injected myocardium. The mechanisms by which VEGF-A stimulated revascularization and recruited cardiomyocyte-like cells were not determined.

Collectively, the studies on VEGF-A-driven neovascularization support the conclusion that the length and height of the VEGF-A "pulse" must be optimized in order to produce functional blood vessels in situ without untoward effects. The intensity and duration of VEGF-A expression varies among different expression systems, and these properties were important determinants of the number and function of newly formed vessels. Prolonged expression of VEGF-A, most pronounced with adenoviral expression vectors, appears to upset the appropriate balance between paracrine factors responsible for formation of mature vessels. Optimizing the length of the "pulse" of VEGF-A expression might then correct this balance and produce more mature vessels^{63, 70-73}. Our study shows that modified RNA technology is a novel and efficient myocardial gene transfer platform with characteristics that are well suited to achieving efficacious VEGF-A delivery.

2. Supplemental Tables

Suppl. Table 1: Selected animal studies of cardiac revascularization with VEGF-A

Species	Study	Delivery Method	Outcome
Mouse	Webber et al ⁷⁴ . 2010.	Recombinant protein (VEGF-A ₁₆₅) and nanofibers, direct intramyocardial injection	Improved ventricular contractile function
	Su et al ⁵⁹ . 2004.	Hypoxia-inducible adenoviral vector (VEGF-A ₁₆₅), intramyocardial injection	Neovascularization, smaller infarct size, and improved ventricular contractile function observed
Rat	Schwarz et al ⁶³ . 2001.	Non-viral vector (VEGF-A ₁₆₅), intramyocardial injection	Neovascularization without increase in measured myocardial blood flow, angiomas noted at injection site
Rabbit	Yockman et al ⁶¹ . 2009.	Hypoxia-inducible, non-viral vector (VEGF ₁₆₅), intramyocardial injection	Neovascularization and reduction in infarct size noted
	Wright et al ⁶² . 2001.	Adenoviral, HSV and non-viral constructs used to express reporter genes, intramyocardial injection	Adenoviral vector associated with marked inflammation, whereas non-viral construct was not
Sheep	Vera Janavel et al ⁶⁵ . 2012.	Non-viral vector (VEGF ₁₆₅), Intramyocardial injection	Neovascularization with reduction in infarct size and improvement in ventricular function, no inflammation
Dog	Banai et al ⁷⁵ . (1994)	Recombinant VEGF-A protein, intramyocardial injection	Neovascularization observed, no change in ventricular function
Pig	Lin et al ⁶⁸ . (2012)	Recombinant protein (VEGF ₁₆₅) and peptide-based nanofibers, direct intramyocardial injection	Increased capillary density and improved ventricular function
	Hughes et al ⁷⁶ . (2004)	Recombinant protein (VEGF ₁₆₅), intravenous and intramyocardial injection	Improved ventricular perfusion
	Rutanen et al ⁵⁸ . (2004)	Adenoviral vector (VEGF-D _{DND} C and VEGF ₁₆₅), intramyocardial injection with NOGA catheter	Increased myocardial perfusion, increased vascular permeability with tissue edema
	Sato et al ⁷⁷ . (2001)	Recombinant protein (VEGF ₁₆₅), intravenous and intracoronary injection	Hypotension associated with injection, greater degree of neovascularization with intracoronary injection, improved myocardial perfusion noted in intracoronary but not intravenous group
	Kornowski et al ⁷⁸ . (2000)	Adenoviral vector and recombinant protein (VEGF ₁₂₁), intramyocardial injection	Neovascularization observed in both groups
	Tio et al ⁶⁰ . (1999)	Non-viral plasmid (VEGF ₁₆₅), intramyocardial injection	Neovascularization observed with coronary angiography
	Lopez et al ⁷⁹ . (1998)	Recombinant protein (VEGF ₁₆₅), intracoronary injection and epicardial osmotic delivery	Neovascularization observed, with evidence of increased coronary blood flow with adenosine challenge

Suppl. Table 2: Selected, placebo-controlled clinical trials of cardiac revascularization with VEGF-A

Study	# Patients	Study Design	Delivery Method	Outcome
REVASC Trial, Stewart et al. ⁸⁰ (2006)	67	Unblinded, no placebo	Adenoviral VEGF ₁₂₁ expression vector, intramyocardial injection	No improvement in myocardial perfusion (26 week follow-up)
Euroinject One Trial, Kastrup et al. ⁸¹ (2005)	80	Double-blind, placebo-controlled	Adenoviral VEGF ₁₆₅ expression vector, intramyocardial injection	No improvement in ventricular perfusion or function (3 month follow-up)
VIVA Trial, Henry et al. ⁸² (2003)	178	Double-blind, placebo-controlled	Recombinant VEGF ₁₆₅ protein, intracoronary infusion	No improvement in ventricular function (60 day follow-up)
KAT Trial, Hedman et al. ⁸³ (2003)	103	Double-blind, placebo-controlled	Adenoviral VEGF ₁₆₅ expression vector, intracoronary infusion	Improved myocardial perfusion (6 month follow-up)

Suppl. Table 3: Summary of the differences between DNA or modRNA delivery to the heart.

Parameter	DNA delivery	modRNA Delivery
Kinetics	Broad peak	Pulse - like
Peak expression	72 hours	18 hours
Time until below 10% of maximum expression	>2 weeks	4 days
Transfection level	Sparse transfection	Frequent transfection
Genomic modification	Infrequent	No
Innate immunity response	elicit	Not elicit

Suppl. Table 4: Open reading frame sequences used for modRNA production

Name	Sequence
GFP	atggtgagcaagggcgaggagctgttcaccgggggtggtgcccatcctggtcgagctggacgg cgacgtaaaccggccacaagttcagcgtgtccggcgagggcgagggcgatgccacctacggca agctgacctgaagttcatctgcaccaccggcaagctgcccgtgccctggcccacctcgtg accacctgacctacggcgtgcagtgttcagccgctaccccgaccacatgaagcagcacga cttcttcaagtccgccatgccgaaggctacgtccaggagcgcaccatcttcttcaaggacg acggcaactacaagaccgcgcgcgaggtgaagttcgagggcgacacctggtgaaccgcac gagctgaagggcatcgacttcaaggaggacggcaacatcctggggcacaagctggagtacaa ctacaacagccacaacgtctatatcatggccgacaagcagaagaacggcatcaaggtgaact tcaagatccgccacaacatcgaggacggcagcgtgcagctcgcggaccactaccagcagaac acccccatcggcgacggccccgtgctgctgcccgacaaccactacctgagcaccagtcgcg cctgagcaaagaccccaacgagaagcgcgatcacatggtcctgctggagttcgtgaccgccg ccgggatcactctcggcatggacgagctgtacaagtaa
Nuclear GFP	atggtgagcaagggcgaggagctgttcaccgggggtggtgcccatcctggtcgagctggacgg cgacgtaaaccggccacaagttcagcgtgtccggcgagggcgagggcgatgccacctacggca agctgacctgaagttcatctgcaccaccggcaagctgcccgtgccctggcccacctcgtg accacctgacctacggcgtgcagtgttcagccgctaccccgaccacatgaagcagcacga cttcttcaagtccgccatgccgaaggctacgtccaggagcgcaccatcttcttcaaggacg acggcaactacaagaccgcgcgcgaggtgaagttcgagggcgacacctggtgaaccgcac gagctgaagggcatcgacttcaaggaggacggcaacatcctggggcacaagctggagtacaa ctacaacagccacaacgtctatatcatggccgacaagcagaagaacggcatcaaggtgaact tcaagatccgccacaacatcgaggacggcagcgtgcagctcgcggaccactaccagcagaac acccccatcggcgacggccccgtgctgctgcccgacaaccactacctgagcaccagtcgcg cctgagcaaagaccccaacgagaagcgcgatcacatggtcctgctggagttcgtgaccgccg ccgggatcactctcggcatggacgagctgtacaagggagatccaaaaaagaagagaaaggt ggcgatccaaaaaagaagagaaaggttaggtgatccaaaaaagaagagaaaggtataa
Luciferase	atggccgatgctaagaacattaagaagggccctgctcccttctaccctctggaggatggcac cgctggcgagcagctgcacaaggccatgaagaggtatgccctggtgcctggcaccattgcct tcaccgatgccacattgaggtggacatcacctatgccgagtacttcgagatgtctgtgcgc ctggccgagggccatgaagaggtacggcctgaacaccaaccaccgcacgtggtgtgctctga gaactctctgcagttcttcatgccagtgtgggcgcctgttcacggagtgccgtggccc ctgctaacgacattttacaacgagcgcgagctgctgaacagcatgggcatttctcagcctacc gtggtgttctgtgtctaagaagggcctgcagaagatcctgaacgtgcagaagaagctgcctat catccagaagatcatcatcatggactctaagaccgactaccagggttccagagcatgtaca cattcgtgacatctcatctgcctcctggcttcaacgagtacgacttcgtgccagagtctttc gacagggacaaaaccattgcccctgatcatgaacagctctgggtctaccggcctgcctaaggg cgtggccctgcctcatcgaccgcctgtgtgctgttctctcacgcccgcgaccctattttcg gcaaccagatcatccccgacaccgctattctgagcgtggtgccattccaccacggcttcggc atgttcaccaccctgggtacctgatttgccgttttcgggtggtgctgatgtaccgcttcga ggaggagctgttctctgcgcagcctgcaagactacaaaattcagctctgcctgctggtgccaa ccctgttcagcttcttcgctaagagcaccctgatcgacaagtagcactgtctaacctgcac gagattgcctctggcggcgccccactgtctaaggaggtgggcgaagcgtggccaagcgctt tcatctgccaggcatccgccagggtacggcctgaccgagacaaccagcgcattctgatta ccccagagggcgacgacaagcctggcgccgtgggcaaggtggtgccattcttcgaggccaag gtggtggacctggacaccggcaagaccctgggagtgaccagcgcggcgagctgtgtgtgcg cgccctatgattatgtccggctacgtgaataaccctgaggccacaaacgcctgatcgaca aggacggctggctgcactctggcgacattgcctactgggacgaggacgagcacttcttcac gtggaccgcctgaagtctctgatcaagtacaagggctaccaggtggccccagccgagctgga gtctatcctgctgcagcaccctaacatttttcgacgccggagtggccggcctgcccgacgacg

	atgccggcgagctgcctgccgccgtcgtcgtgctggaacacggcaagaccatgaccgagaag gagatcgtggactatgtggccagccaggtgacaaccgccaagaagctgcgcggcgagtggt gttcgtggacgaggtgcccaagggcctgaccggcaagctggacgcccgaagatccgcgaga tcctgatcaaggctaagaaaggcggaagatcgccgtgtaa
Cre Recombinase	atgtccaatttactgaccgtacacaaaatttgcctgcattaccggtcgatgcaacgagtga tgaggttcgaagaacctgatggacatgttcagggatcgccaggcgtttctgagcatacct ggaaaatgcttctgtccgtttgccggctcgtgggcggcatggtgcaagttgaataaccggaaa tggtttcccgacagaacctgaagatgttcgcgattatcttctatatcttcaggcgcgcggtct ggcagtaaaaaactatccagcaacatttggggcagctaaacatgcttcacatcgtcgggtccgggc tgccacgaccaagtgcagcaatgctgtttcactggttatgcggcggatccgaaaagaaaac gttgatgccgggtgaacgtgcaaaacaggctctagcgttcgaacgcactgatttcgaccaggt tcgttcactcatggaataatagcgatcgtgccaggatatacgtaatctggcatttctgggga ttgcttataacaccctgttacgtatagccgaaattgccaggatcagggttaaagatatctca cgtactgacgggtgggagaatgttaatccatattggcagaacgaaaacgctgggttagcaccgc aggtgtagagaaggcacttagcctgggggtaactaaactggtcgagcgatggatttccgtct ctggtgtagctgatgatccgaataactacctgttttgccgggtcagaaaaaatggtgttgcc gcgccatctgccaccagccagctatcaactcgcgccttgaagggatttttgaagcaactca tcgattgatttacggcgctaaggatgactctggtcagagataacctggcctggtctggacaca gtgcccggtgtcggagccgcgcgagatatggcccgctggagtttcaataccggagatcatg caagctggtggctggaccaatgtaaatattgtcatgaactatatccgtaacctggatagtga aacaggggcaatggtgcgcctgctagaagatggcgattag
human VEGF-A ₁₆₅	atgaactttctgctgtcttgggtgcattggagccttgccttgctgctctacctccaccatgc caagtgggtcccaggctgcacccatggcagaaggaggaggcagaatcatcacgaagtgggtga agttcatggatgtctatcagcgcagctactgccatccaatcgagacctgggtggacatcttc caggagtaccctgatgagatcgagtacatcttcaagccatcctgtgtgccctgatgcgatg cgggggctgctgcaatgacgagggcctggagtgtgtgccactgaggagtccaacatacca tgcagattatgcggtatcaaacctaccaaggccagcacataggagagatgagcttcctacag cacaacaaatgtgaatgcagaccaaagaaagatagagcaagacaagaaaatccctgtgggcc ttgctcagagcggagaaaagcatttgtttgtacaagatccgcagacgtgtaaatgttcctgca aaaacacagactcgcgttgcaaggcgaggcagcttgagttaaacgaacgtacttgcagatgt gacaagccgaggcggtga

Suppl. Table 5: Antibodies used in this study

Name	Company
70 kD FITC-dextran beads	Sigma
Annexin V	eBiosciences
β -Galactosidase	Abcam
TNNT2	NeoMarkers
α -Actinin	Abcam
VE-Cadherin	Abcam
SMMHC	Abcam, Biomedical Technologies, Inc.
Isolectin B4	Vector Lab
WT1	Abcam, Calbiochem
PECAM1	Abcam, BD biosciences
Vimentin	R&D systems
TNNI3	BD ebiosciences
TUNEL	Roche
KDR	R&D systems
Anti - GFP	Invitrogen
Alexa-488	Invitrogen
Alexa-594	Invitrogen
Alexa-650	Invitrogen
DAPI	Sigma

Suppl. Table 6: Primer Sequences

Genes	Forward	Reverse
<i>Gapdh</i>	ttgtctcctgcgacttcaac	gtcataccaggaaatgagcttg
<i>Actb</i>	aggtgacagcattgcttctg	gctgcctcaacacctcaac
<i>Pecam1</i>	ctgccagtcgaaaaatggaac	cttcatccaccggggctatc
<i>Tnnt2</i>	ctgagacagaggaggccaac	ttccgctctgtcttctggat
<i>Kdr</i>	agaacacccaaaagagagaggaacg	gcacacaggcagaaaccagtag
<i>Vim</i>	gacattgagatcgccaccta	ggcagagaaaatcctgctctc
<i>Tcf21</i>	cattcaccagtcacacctga	ccacttccttcaggctattctc
<i>Wt1</i>	agacacacaggtgtgaaacca	atgagtcctggtgtgggtct
<i>Isl1</i>	agcaccagcatcctctctgt	tgaagcctatgctgcacttg
<i>Infα</i>	atggctagrcctctgtgctttcct	agggctctccagayttctgctctg
<i>Infβ</i>	aagagttacactgcctttgccatc	cactgtctgctggtggagttcatc
<i>Rig1</i>	ggacgtggcaaaacaaatcag	gcaatgtcaatgccttcatca
<i>Smmhc</i>	aagctgcggttagaggtca	ccctccctttgatggctgag
<i>Nkx2-5</i>	ccagtctgggtcctaatacggggtggcgtct	gatagggcctttttaaatagctccgagttt
<i>hVEGF-A</i>	aaggaggagggcagaatcat	ccaggccctcgtcattg
<i>VEGF-A</i>	ctgtgcaggtgctgtaacg	gttcccgaaccctgaggag
<i>Vegfb</i>	cccctgtgtcccagtttg	cgtctatccatggcaccac
<i>Vegfc</i>	cagacaagttcattcaattattagacg	catgtcttgtagctgcctga
<i>Vegfd</i>	gcaactttctatgacactgaaacac	tctctctagggctgcattgg
<i>Plgf</i>	aggcagaaaggaggaaaacc	gttacctccgggaaatgaca

3. Supplemental Methods

Experimental MI model. All surgical and experimental procedures with mice were performed in accordance with protocols approved by Institutional Animal Care and Use Committees at Massachusetts General Hospital or Children's Hospital Boston. CFW, C57Bl/6, R26fs^{LacZ}, WT1^{GFP^{Cre}/+} or WT1^{CreERT2/+}::R26^{mTmG} mice (6-8 weeks old) were anesthetized with isoflurane. MI was induced by permanent ligation of the LAD, as previously described⁸⁴. Briefly, the left thoracic region was shaved and sterilized. After intubation, the heart was exposed through a left thoracotomy. A suture was placed to ligate the LAD. The thoracotomy and skin were sutured closed in layers. Excess air was removed from the thoracic cavity, and the mouse was removed from ventilation when normal breathing was established. In order to determine the effect of hVEGF-A modRNA in cardiovascular outcome after MI, lipofectamine vehicle, hVEGF-A modRNA (100 µg/heart) or hVEGF-A DNA (100 µg/heart) were injected into the infarct zone immediately after LAD ligation. Sham controls were the same as the MI operation but without LAD ligation. Where indicated, DMSO or VEGF receptor inhibitors (0.5 mg/mouse IP) were administered daily from one day before to seven days after MI. Inhibitors used were SU5614 (Sigma) or PTK787 (Selleckchem). In short term survival experiments mice that were injected with VEGF-A modRNA or DNA after MI we treated twice a week with humanized anti-VEGF monoclonal antibody (Avastin, a kind gift from Dr. David Briscoe) for four weeks. For analysis, the peri-infarct zone near the apex was either snap-frozen for RNA isolation and subsequent real-time qPCR studies, or was fixed in 4% PFA for cryosectioning and immunostaining. For Cre gel experiments, the gel was delivered through a lower intercostal space than that used for LAD ligation two weeks later. In all experiments, the surgeon was blinded to treatment group.

To obtain a 3 dimensional cast of the vasculature, a ligature was placed on the aorta and yellow MicroFil® (Flow Tech, Inc) was injected proximally to fill and opacify the coronary vasculature. Hearts were cleared by washing through an ethanol-methyl salicylate series (25% for 1 day, 50% for 1 day, 75% for 1 day, 92% for 2 days, 100% for 1 day). To examine the localization of X-gal⁺ cells, X-gal (Fermentas) staining was performed according to manufacturer's instruction. To examine the degree of fibrosis, short-axis slices of the heart were created at defined intervals from the apex to the base of the left ventricle. These slices were stained with Masson's trichrome (Leica) according to the manufacturer's instructions. In each slice, areas of fibrosis (revealed by blue staining) were measured with the UTHSCSA ImageTool software package⁸⁵.

Detection of luciferase⁺ cells in vivo using the IVIS system. Vehicle (a mixture of 75 µl RNAiMAX and 5 µl opti-MEM basal medium) or luc modRNA (100 µg/heart) was administered intramuscularly into the left ventricle of hearts of Balb/c mice or skeletal muscle (biceps femoris) of CFW mice. Bioluminescence imaging of the injected mice was taken at different time points (3-240 hours) which each unit represent p/sec/cm2/srX10⁶ (Luc signal). To visualize Luc⁺ cells, luciferin (150 µg/g body weight; Sigma) was injected intraperitoneally. After 10 minutes, mice were anesthetized with isoflurane (Abbott Laboratories), and imaged using an IVIS100 charge-coupled device imaging system for 2 minutes. Imaging data were analyzed and quantified with Living Image Software. The strength of the signal was indicated by the spectrum of different

colors. Hearts or skeletal muscles that were injected with the vehicle only served as baseline for Luc expression.

Magnetic Resonance Imaging (MRI). C57Bl/6 (6-8 week old) treated with vehicle or hVEGF-A modRNA were subjected to MRI assessment at days 1 and 21 after LAD ligation. We obtained delayed-enhancement CINE images on a 7-T Bruker Pharmascan with cardiac and respiratory gating (SA Instruments, Inc, Stony Brook, New York). Where ejection fraction was within the range of 50–60%, follow-up MRI analyses were performed on the same mice at day 21 post-MI to determine temporal changes in infarct size and cardiac function. Mice were anaesthetized with 1-2% isoflurane/air mixture. ECG, respiratory, and temperature probes were placed on the mouse which was kept warmed during scans. Imaging was performed 10 to 20 min after IV injection of 0.3 mmol/kg gadolinium-diethylene triamine pentaacetic acid. A stack of short-axis slices covering the heart from the apex to the base was acquired with an ECG triggered and respiratory-gated FLASH sequence⁸⁶ with the following parameters: echo time (TE) 2.7 msec with resolution of 200 μm x 200 μm ; slice thickness of 1 mm; 16 frames per R-R interval; 4 excitations with flip angle at 60°. Eight to ten short-axis slices were acquired from the apex to the base to cover the left ventricle. Ejection fraction was calculated as the difference in end-diastolic and end-systolic volumes, divided by the end-diastolic volume. MRI acquisition and analyses were performed blinded to treatment group.

RNA isolation and gene expression profiling. Total RNA was isolated using the RNeasy mini kit (Qiagen) and reverse transcribed using Superscript III reverse transcriptase (Invitrogen), according to the manufacturer's instructions. Real-time qPCR analyses were performed on a Mastercycler realplex 4 Sequence Detector (Eppendorf) using SYBR Green (QuantitectTM SYBR Green PCR Kit, Qiagen). Data were normalized to *Gapdh* or *Actb* expression, where appropriate (endogenous controls). Fold-changes in gene expression were determined by the $\Delta\Delta\text{CT}$ method and were presented relative to an internal control. PCR primer sequences are shown in Supplementary Table 6. To characterize GFP⁺ progenitors, total RNA was obtained from FACS-sorted GFP⁺ cells, isolated after collagenase digestion of the vehicle-treated or the hVEGF-A modRNA-treated hearts derived from WT1^{GFP^{Cre}/+} or WT1^{CreERT2/+::R26^{mTmG}} mice 7 days post MI using a FACSaria III cell sorter. To examine the expression level of *Wt1* among different tissues, bone marrow, spleen, heart and blood cells were isolated from CFW mice injected with VEGF-A modRNA (100 μg) or vehicle.

Myotube differentiation and transfection. Skeletal muscle myotubes were differentiated from primary mouse satellite cells. Satellite cell isolation was performed as previously described^{87, 88}. Briefly, myofiber associated (MFA) cells were prepared from intact skeletal muscles (Extensor digitorum longus, gastrocnemius, quadriceps, soleus, tibialis anterior, triceps brachii, abdominal) by digesting the muscles with collagenase type II and then dispase enzymes. MFA cells were stained for isolation of CD45- Sca-1- Mac-1- CXCR4+ β 1-integrin+ cells by fluorescence activated cell sorting (FACS). Isolated cells were seeded on collagen/laminin-coated plates in F10 medium (Gibco) containing 20% horse serum (Atlanta Biologics), 1% penicillin-streptomycin (Invitrogen) and 1% glutamax (Invitrogen). 5 ng/ml bFGF (Sigma) was added to the media daily and cells were expanded for 5 days. On day 5, cells were harvested and equal numbers (8000

cells) were re-plated in each well of a 96-well plate in growth media. Media was changed to DMEM (gibco), containing 2% horse serum (Atlanta Biologics) and 1% penicillin-streptomycin (myotube differentiation media) after 12 hours. Cells were transfected with modified RNA after 3 days in differentiation media. Myotubes were transfected with 0, 0.3, 1 or 3 μg of GFP modified RNA using lipofectamine RNAiMax transfection reagent (Invitrogen) according to the manufactures instruction. Transfection reagent was changed to myotube differentiation media after 6 hours and cells were fixed 16 hours after transfection. Transfected myotubes were stained for skeletal muscle myosin heavy chain (Primary antibody: anti-skeletal myosin type II (fast- twitch) 1:200 and anti-skeletal myosin type I (slow-twitch) 1:100, Sigma. Secondary: goat anti-mouse IgG Alexa-555 conjugate (Molecular Probes) 1:250), 10 $\mu\text{g}/\text{ml}$ Hoechst (Invitrogen) and rabbit anti-GFP Alexa-488 1:200 (invitrogen). Pictures were taken from the whole well using the Celigo cytometer (Cyntellect) under blue, red and green channels. Cell viability was measured by quantifying the total number of nuclei in the transfected wells 16 hours after transfection and normalizing them to the total number of nuclei in the non-transfected wells. Total number of nuclei in the whole wells was quantified using a modified ImageJ macro.

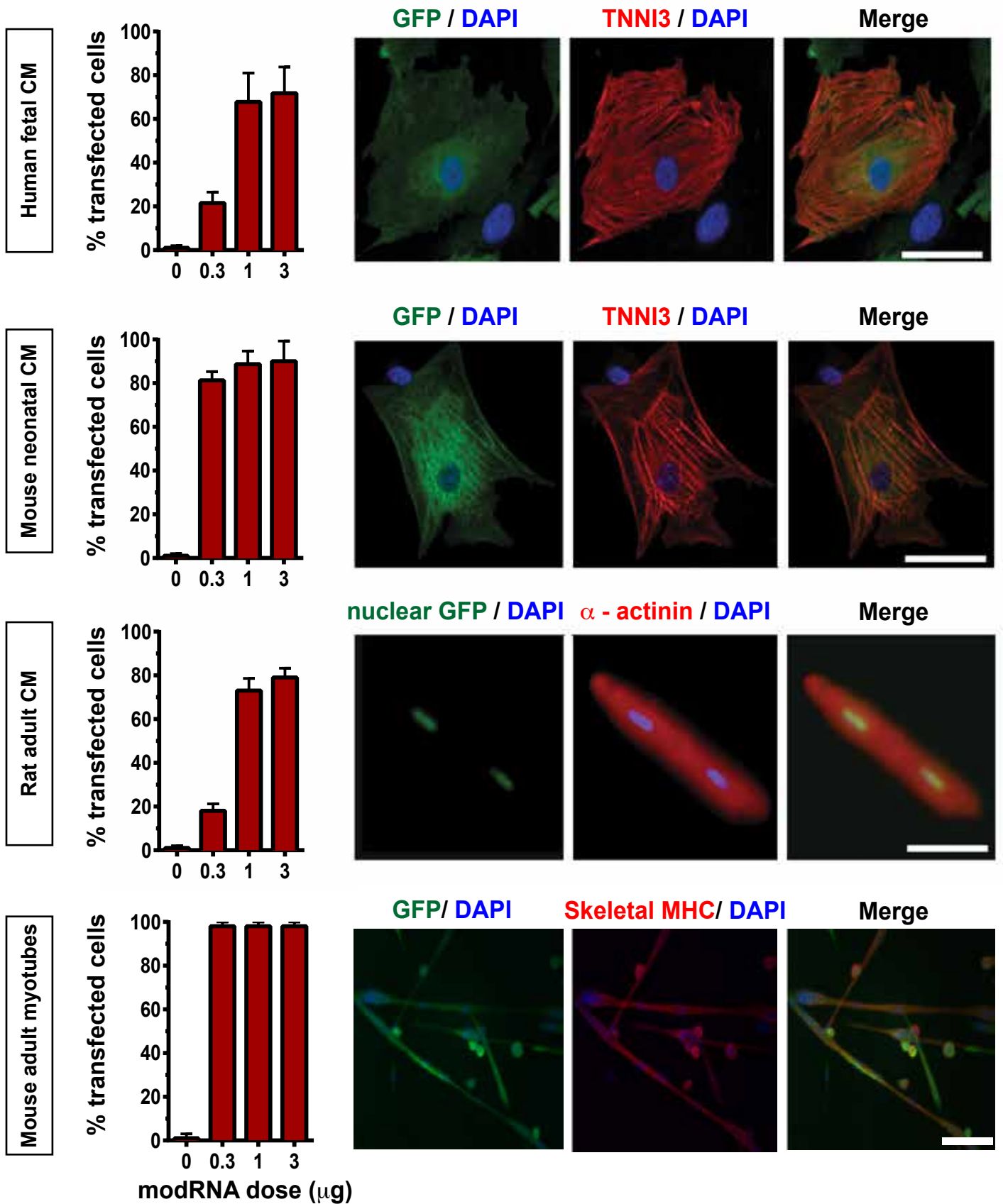
4. Supplemental References

48. Ferrara, N. et al. Heterozygous embryonic lethality induced by targeted inactivation of the VEGF gene. *Nature* **380**, 439-442 (1996).
49. Riley, P.R. & Smart, N. Vascularizing the heart. *Cardiovascular research* **91**, 260-268 (2011).
50. Levy, A.P., Levy, N.S., Wegner, S. & Goldberg, M.A. Transcriptional regulation of the rat vascular endothelial growth factor gene by hypoxia. *The Journal of biological chemistry* **270**, 13333-13340 (1995).
51. Carmeliet, P. Angiogenesis in life, disease and medicine. *Nature* **438**, 932-936 (2005).
52. Carmeliet, P. et al. Impaired myocardial angiogenesis and ischemic cardiomyopathy in mice lacking the vascular endothelial growth factor isoforms VEGF164 and VEGF188. *Nat Med* **5**, 495-502 (1999).
53. Li, J. et al. VEGF, flk-1, and flt-1 expression in a rat myocardial infarction model of angiogenesis. *The American journal of physiology* **270**, H1803-1811 (1996).
54. Li, J., Hampton, T., Morgan, J.P. & Simons, M. Stretch-induced VEGF expression in the heart. *The Journal of clinical investigation* **100**, 18-24 (1997).
55. Stefanini, M.O., Wu, F.T., Mac Gabhann, F. & Popel, A.S. The presence of VEGF receptors on the luminal surface of endothelial cells affects VEGF distribution and VEGF signaling. *PLoS Comput Biol* **5**, e1000622 (2009).
56. Yang, R. et al. Exaggerated Hypotensive Effect of Vascular Endothelial Growth Factor in Spontaneously Hypertensive Rats. *Hypertension* **39**, 815-820 (2002).
57. Henry, T.D. et al. Intracoronary administration of recombinant human vascular endothelial growth factor to patients with coronary artery disease. *American heart journal* **142**, 872-880 (2001).
58. Rutanen, J. et al. Adenoviral catheter-mediated intramyocardial gene transfer using the mature form of vascular endothelial growth factor-D induces transmural angiogenesis in porcine heart. *Circulation* **109**, 1029-1035 (2004).
59. Su, H. et al. Adeno-associated viral vector delivers cardiac-specific and hypoxia-inducible VEGF expression in ischemic mouse hearts. *Proceedings of the National Academy of Sciences of the United States of America* **101**, 16280-16285 (2004).
60. Tio, R.A. et al. Intramyocardial gene therapy with naked DNA encoding vascular endothelial growth factor improves collateral flow to ischemic myocardium. *Human gene therapy* **10**, 2953-2960 (1999).
61. Yockman, J.W. et al. Polymeric gene delivery of ischemia-inducible VEGF significantly attenuates infarct size and apoptosis following myocardial infarct. *Gene Ther* **16**, 127-135 (2009).
62. Wright, M.J. et al. In vivo myocardial gene transfer: optimization, evaluation and direct comparison of gene transfer vectors. *Basic research in cardiology* **96**, 227-236 (2001).
63. Schwarz, E.R. et al. Evaluation of the effects of intramyocardial injection of DNA expressing vascular endothelial growth factor (VEGF) in a myocardial infarction model in the rat--angiogenesis and angioma formation. *Journal of the American College of Cardiology* **35**, 1323-1330 (2000).
64. Ylä-Herttuala, S., Rissanen, T.T., Vajanto, I. & Hartikainen, J. Vascular endothelial growth factors: biology and current status of clinical applications in cardiovascular medicine. *Journal of the American College of Cardiology* **49**, 1015-1026 (2007).
65. Vera Janavel, G.L. et al. Effect of vascular endothelial growth factor gene transfer on infarct size, left ventricular function and myocardial perfusion in sheep after 2 months of coronary artery occlusion. *J Gene Med* **14**, 279-287 (2012).
66. Favaloro, L. et al. High-dose plasmid-mediated VEGF gene transfer is safe in patients with severe ischemic heart disease (Genesis-I). A phase I, open-label, two-year follow-

- up trial. *Catheterization and cardiovascular interventions : official journal of the Society for Cardiac Angiography & Interventions* (2012).
67. Ye, L. et al. Nanoparticle based delivery of hypoxia-regulated VEGF transgene system combined with myoblast engraftment for myocardial repair. *Biomaterials* **32**, 2424-2431 (2011).
 68. Lin, Y.-D. et al. Instructive nanofiber scaffolds with VEGF create amicroenvironment for arteriogenesis and cardiac repair. *Sci Transl Med* **4**, 146ra109 (2012).
 69. Tafuro, S. et al. Inducible adeno-associated virus vectors promote functional angiogenesis in adult organisms via regulated vascular endothelial growth factor expression. *Cardiovascular research* **83**, 663-671 (2009).
 70. Olea, F.D. et al. Combined VEGF gene transfer and erythropoietin in ovine reperfused myocardial infarction. *International journal of cardiology* **165**, 291-298 (2013).
 71. Arsic, N. et al. Induction of functional neovascularization by combined VEGF and angiopoietin-1 gene transfer using AAV vectors. *Mol Ther* **7**, 450-459 (2003).
 72. Karvinen, H. et al. Long-term VEGF-A expression promotes aberrant angiogenesis and fibrosis in skeletal muscle. *Gene Ther* **18**, 1166-1172 (2011).
 73. Korpisalo, P. et al. Capillary enlargement, not sprouting angiogenesis, determines beneficial therapeutic effects and side effects of angiogenic gene therapy. *European heart journal* **32**, 1664-1672 (2011).
 74. Webber, M.J. et al. Capturing the stem cell paracrine effect using heparin-presenting nanofibres to treat cardiovascular diseases. *J Tissue Eng Regen Med* **4**, 600-610 (2010).
 75. Banai, S. et al. Angiogenic-induced enhancement of collateral blood flow to ischemic myocardium by vascular endothelial growth factor in dogs. *Circulation* **89**, 2183-2189 (1994).
 76. Hughes, G.C. et al. Therapeutic angiogenesis in chronically ischemic porcine myocardium: comparative effects of bFGF and VEGF. *The Annals of thoracic surgery* **77**, 812-818 (2004).
 77. Sato, K. et al. Efficacy of intracoronary or intravenous VEGF165 in a pig model of chronic myocardial ischemia. *Journal of the American College of Cardiology* **37**, 616-623 (2001).
 78. Kornowski, R. et al. Electromagnetic guidance for catheter-based transendocardial injection: a platform for intramyocardial angiogenesis therapy. Results in normal and ischemic porcine models. *Journal of the American College of Cardiology* **35**, 1031-1039 (2000).
 79. Lopez, J.J. et al. VEGF administration in chronic myocardial ischemia in pigs. *Cardiovascular research* **40**, 272-281 (1998).
 80. Stewart, D.J. et al. Angiogenic gene therapy in patients with nonrevascularizable ischemic heart disease: a phase 2 randomized, controlled trial of AdVEGF(121) (AdVEGF121) versus maximum medical treatment. *Gene Ther* **13**, 1503-1511 (2006).
 81. Kastrup, J. et al. Direct intramyocardial plasmid vascular endothelial growth factor-A165 gene therapy in patients with stable severe angina pectoris A randomized double-blind placebo-controlled study: the Euroinject One trial. *Journal of the American College of Cardiology* **45**, 982-988 (2005).
 82. Henry, T.D. et al. The VIVA trial: Vascular endothelial growth factor in Ischemia for Vascular Angiogenesis. *Circulation* **107**, 1359-1365 (2003).
 83. Hedman, M. et al. Safety and feasibility of catheter-based local intracoronary vascular endothelial growth factor gene transfer in the prevention of postangioplasty and in-stent restenosis and in the treatment of chronic myocardial ischemia: phase II results of the Kuopio Angiogenesis Trial (KAT). *Circulation* **107**, 2677-2783 (2003).

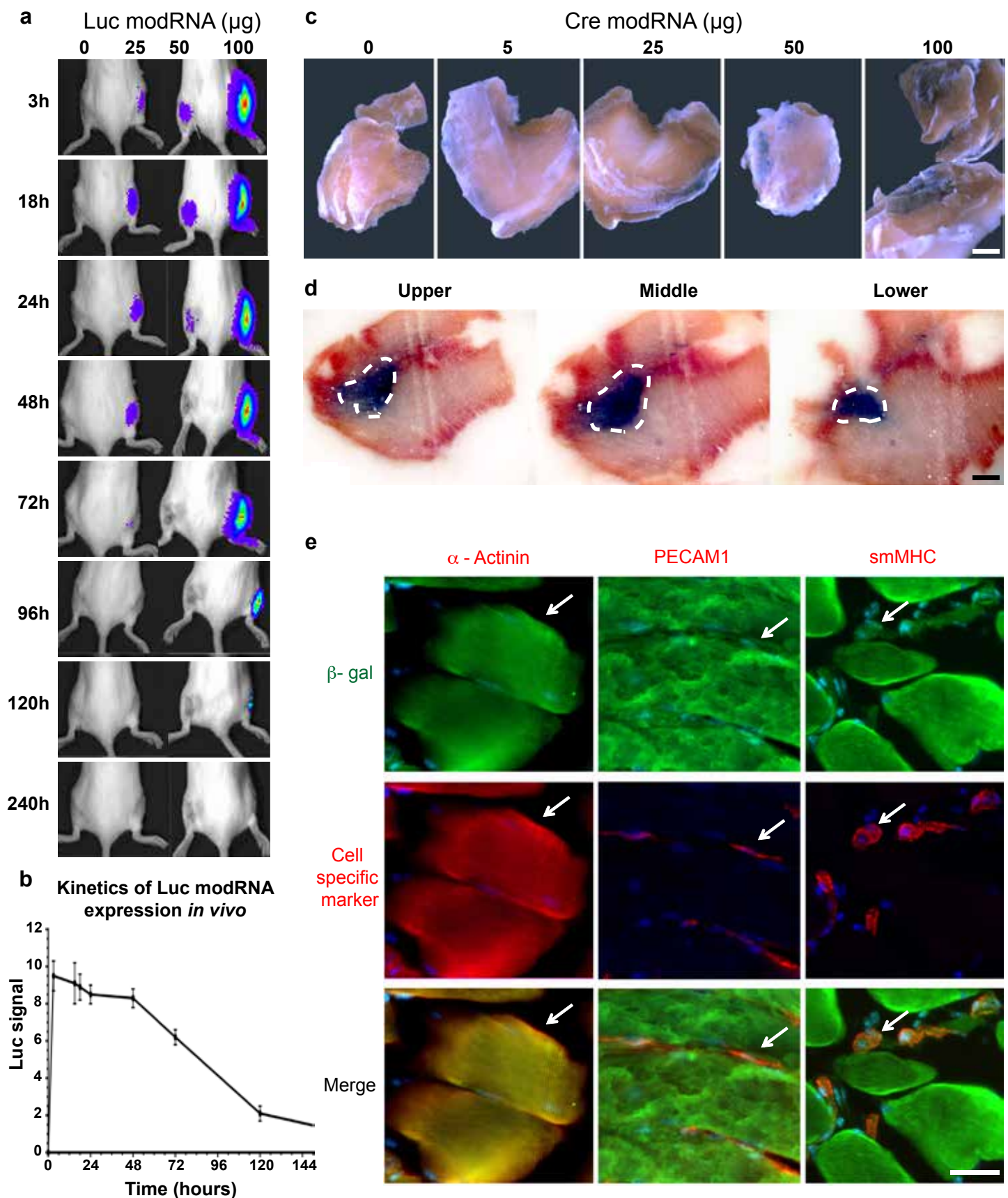
84. Tarnavski, O. et al. Mouse cardiac surgery: comprehensive techniques for the generation of mouse models of human diseases and their application for genomic studies. *Physiol Genomics* **16**, 349-360 (2004).
85. Takagawa, J. et al. Myocardial infarct size measurement in the mouse chronic infarction model: comparison of area- and length-based approaches. *J Appl Physiol* **102**, 2104-2111 (2007).
86. Lee, W.W. et al. PET/MRI of inflammation in myocardial infarction. *Journal of the American College of Cardiology* **59**, 153-163 (2012).
87. Cerletti, M. et al. Highly efficient, functional engraftment of skeletal muscle stem cells in dystrophic muscles. *Cell* **134**, 37-47 (2008).
88. Sherwood, R.I. et al. Isolation of adult mouse myogenic progenitors: functional heterogeneity of cells within and engrafting skeletal muscle. *Cell* **119**, 543-554 (2004).

4. Supplemental Figures



Suppl. Fig. 1. Efficient modRNA-mediated gene transfer to cardiac and skeletal muscles in vitro.

Cytoplasmic or nuclear GFP modRNA was transfected into cultured fetal human, neonatal mouse, and adult rat cardiomyocytes or adult mouse skeletal muscle myotubes. Gene transfer efficiency was determined by immunostaining. Cell viability was not altered by modRNA transfection (~80% viability at all doses and in controls treated with the transfection agent alone). Bars = 20, 20, 50 or 100 µm, respectively.



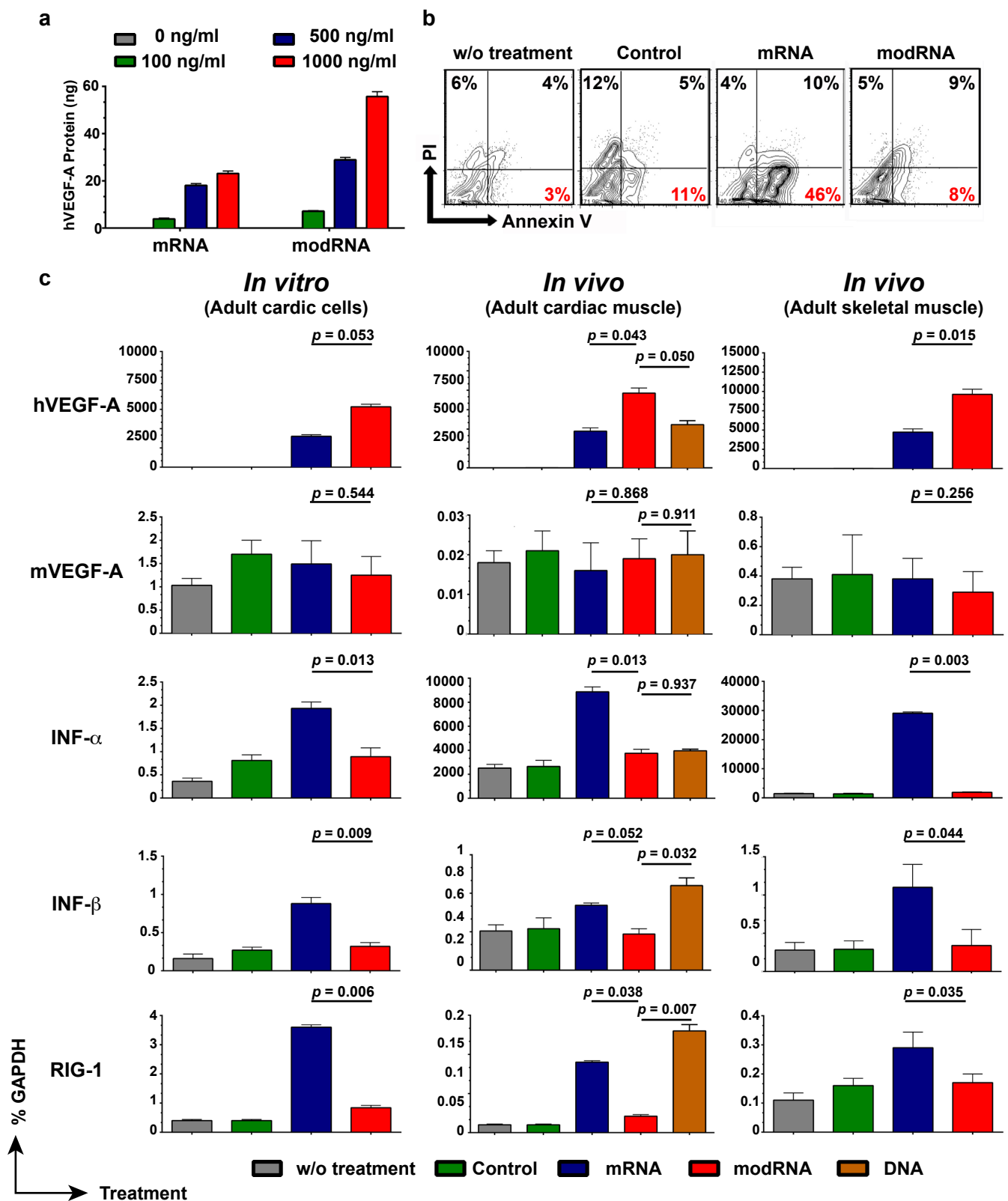
Suppl. Fig. 2. Efficient modRNA-mediated gene transfer to skeletal muscle *in vivo*.

a-b. Indicated amounts of luciferase modRNA were injected into adult mouse skeletal muscle (Biceps femoris) and bioluminescent luciferase activity was measured at the indicated times.

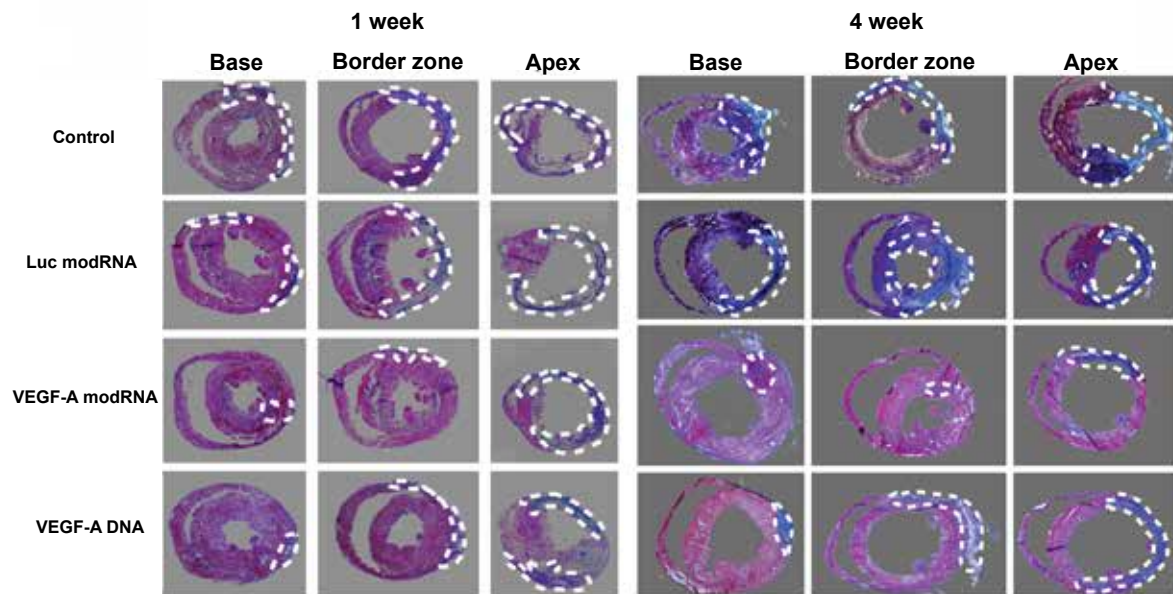
c-d. Cre modRNA (100 μg) was injected into adult R26^{fsLacZ} mouse skeletal muscle (Biceps femoris) and 10 days later Cre-activated LacZ activity was visualized by X-gal staining. c shows whole mount of dissected muscle, and d shows sections through the muscle at different levels.

e. Immunostaining for Cre-activated β -gal and cell specific markers show that Cre modRNA transfected skeletal muscle, endothelial cells, and smooth muscle cells *in vivo*.

Bars = 1 cm, 0.5 mm, and 20 μm in panels c,d, and e, respectively.

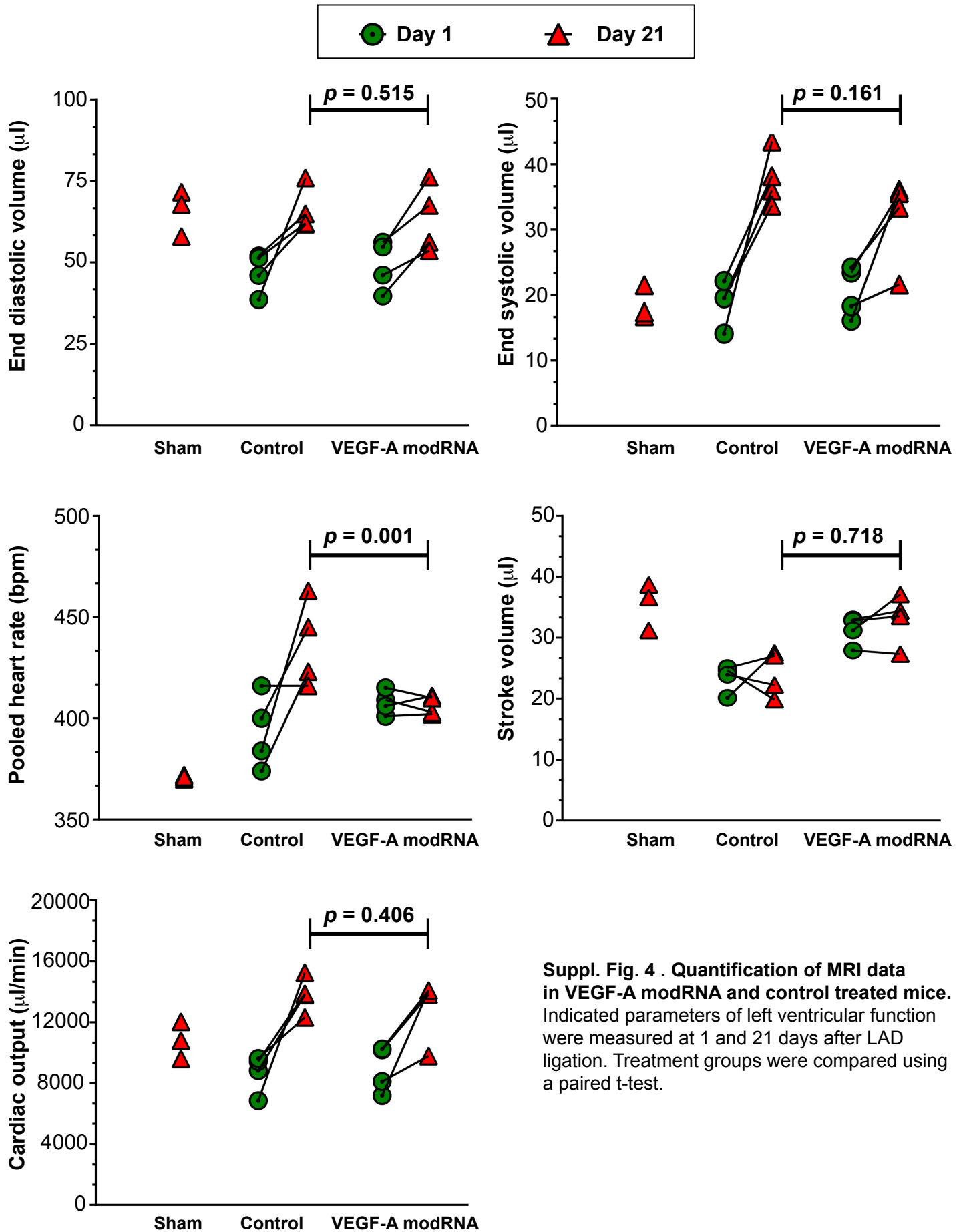


Suppl. Fig. 3. modRNA did not elicit the innate immune response in vitro and in vivo. VEGF-A modRNA or mRNA were transfected into adult cardiac cells. **a.** Efficient translation of VEGF-A mRNA. Cardiac cells were transfected once with VEGF-A modRNA or mRNA. Total secreted VEGF-A protein was collected from cell supernatants over 10 days and measured using ELISA. **b.** Daily transfection with modRNA over three days did not significantly impair cell viability. Viability was measured by Annexin V and PI staining followed by FACS. mRNA strongly increased the apoptotic cell population (Annexin V⁺, PI⁻), while modRNA did not. **c.** modRNA did not significantly activate innate immunity in vitro (adult cardiac cells) or in vivo (cardiac or skeletal muscles). Gene expression was measured by qRT-PCR three days after transfection. Innate immune response markers INFα, INFβ, and RIG1 were upregulated by mRNA but not modRNA. **In addition, VEGF-A DNA plasmid delivery was also tested for his ability to elicit immune response in vivo, and found to activate INFβ and RIG-1.** In vivo measurements were made on tissue from sham-operated animals.

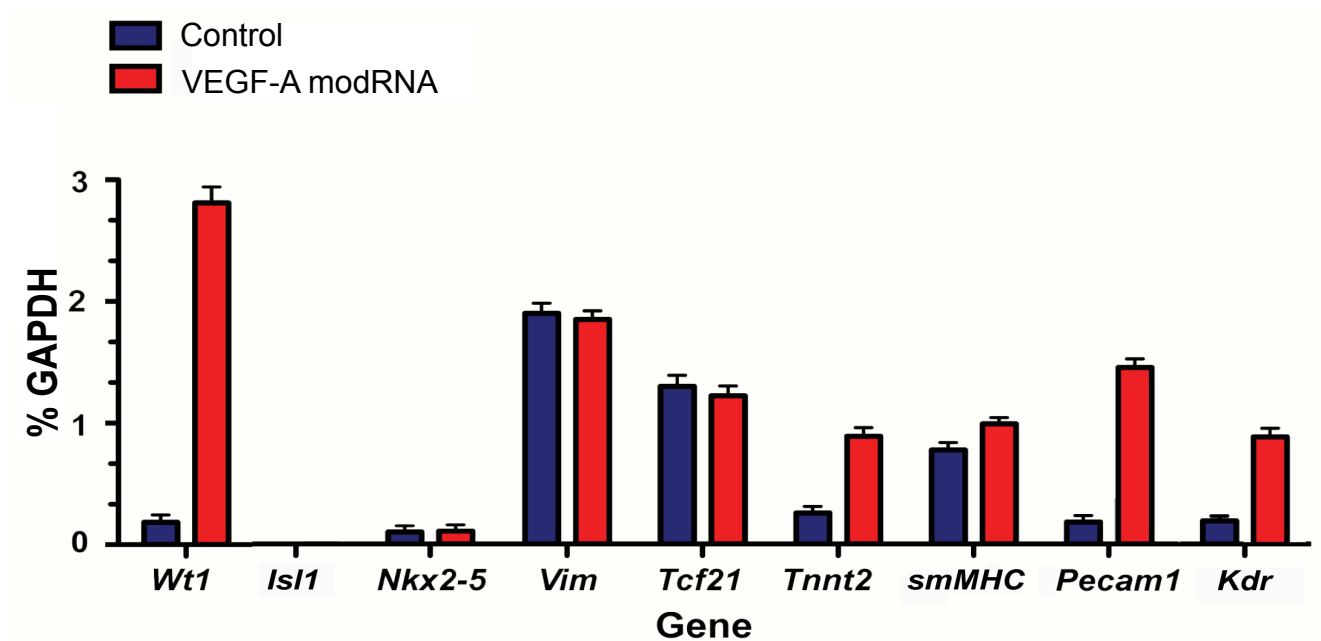


Suppl. Fig. 5 VEGF-A modRNA reduced scar area after MI .

VEGFA modRNA and DNA reduced scar area after MI. Heart sections at regular intervals through the heart were stained by Masson's trichrome stain, which stains scar areas blue. Representative sections are shown, and dotted white lines highlight scar regions with extensive collagen deposition. Quantitative data is shown in Fig. 2e.

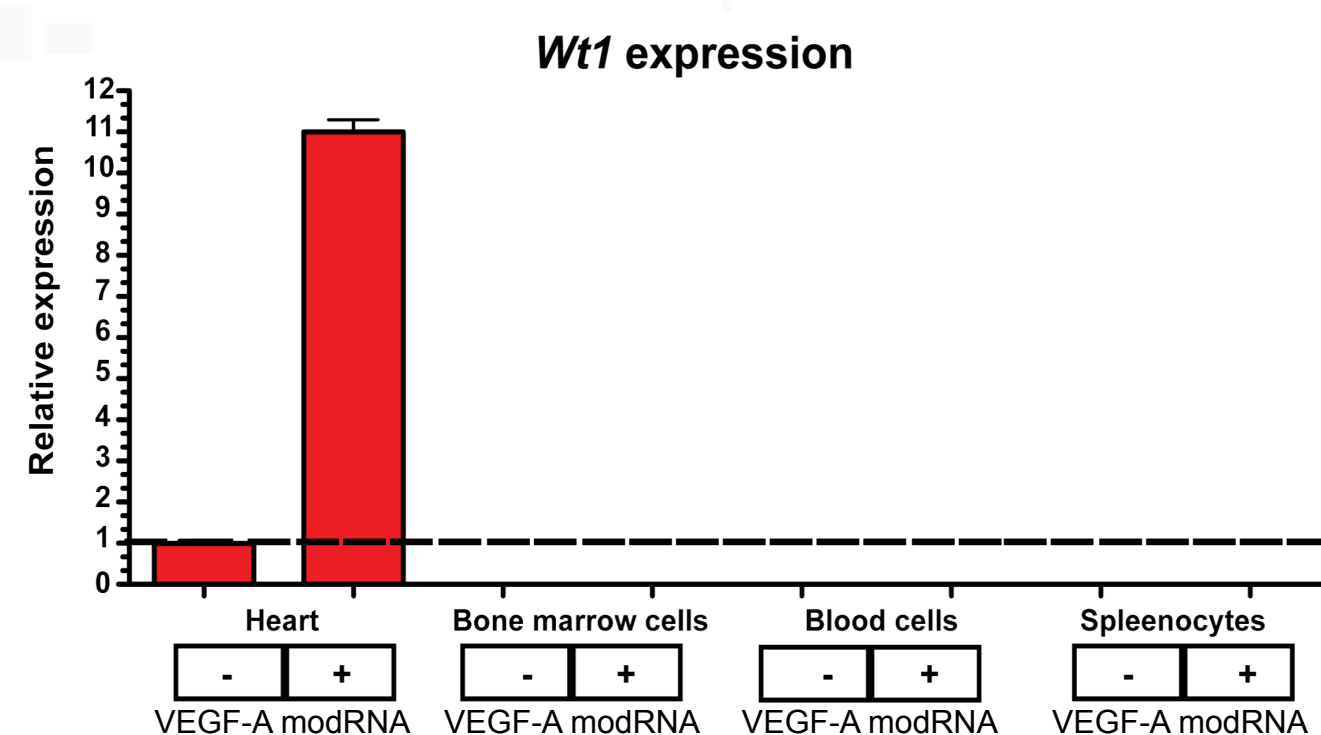


Suppl. Fig. 4 . Quantification of MRI data in VEGF-A modRNA and control treated mice. Indicated parameters of left ventricular function were measured at 1 and 21 days after LAD ligation. Treatment groups were compared using a paired t-test.



Suppl. Fig. 6 VEGF-A modRNA upregulated epicardial and endothelial markers in the peri-infarct region after MI.

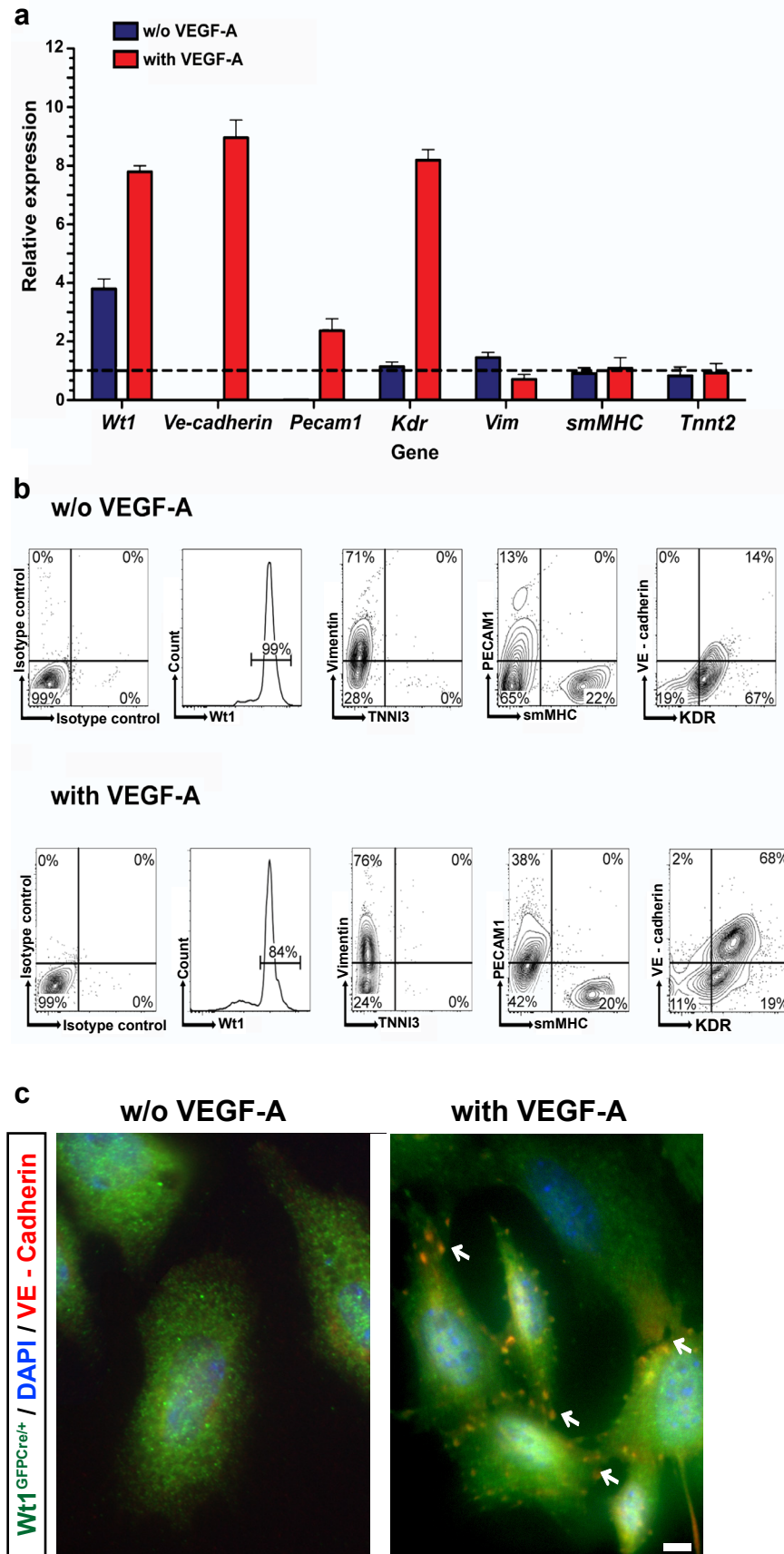
Gene expression in peri-infarct tissue was measured one week after MI and after control or VEGF-A modRNA treatment. Gene expression was calculated as a fraction of GAPDH expression. Note upregulation of *Wt1*, *Pecam1*, and *Kdr* with VEGF-A modRNA treatment.



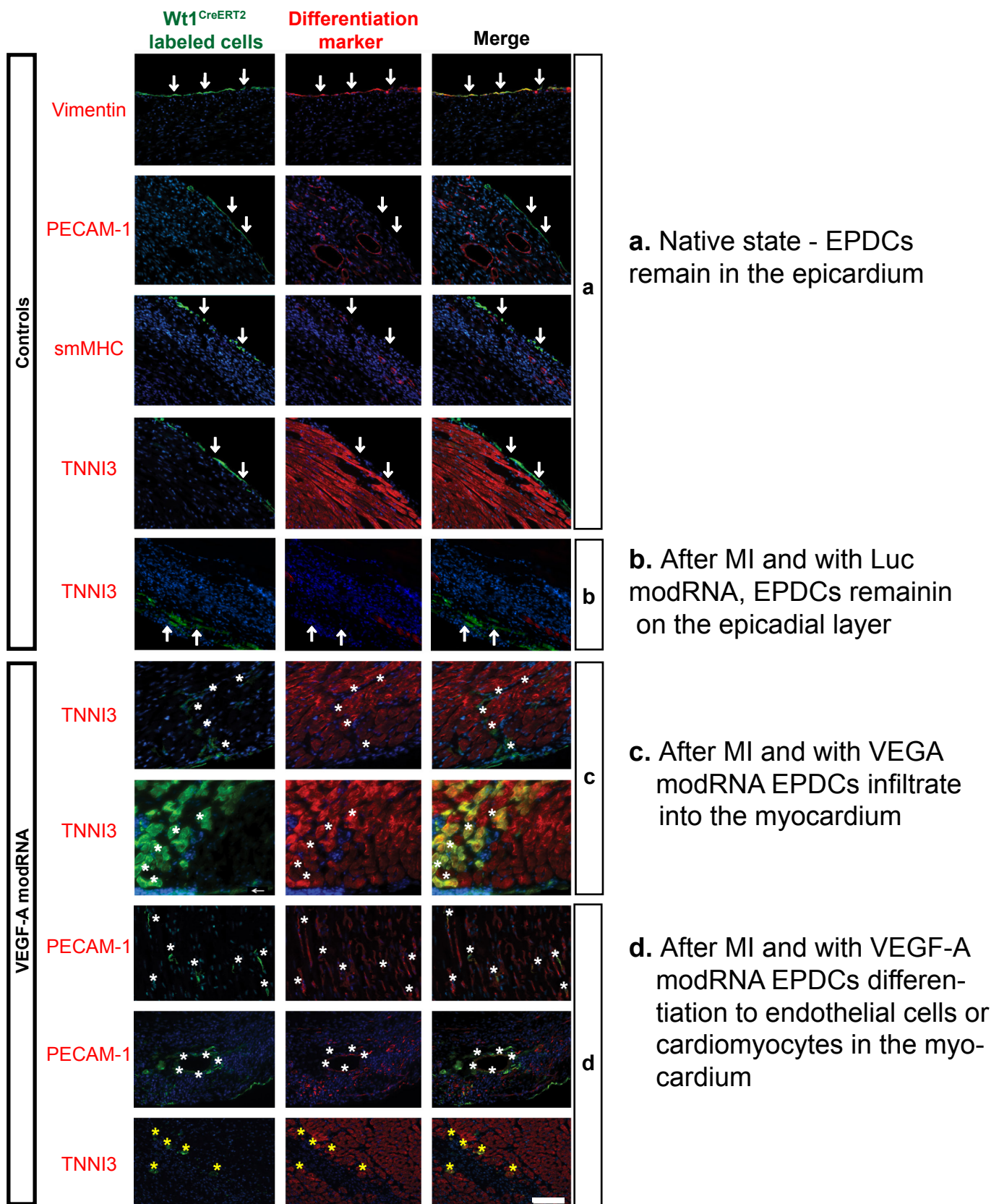
Suppl. Fig. 7 VEGF-A modRNA upregulated *Wt1* expression in heart tissue but not in remote tissues.

VEGF-A modRNA injection into the heart upregulated *Wt1* expression in heart tissue around the injection site but not in remote tissues including blood and bone marrow.

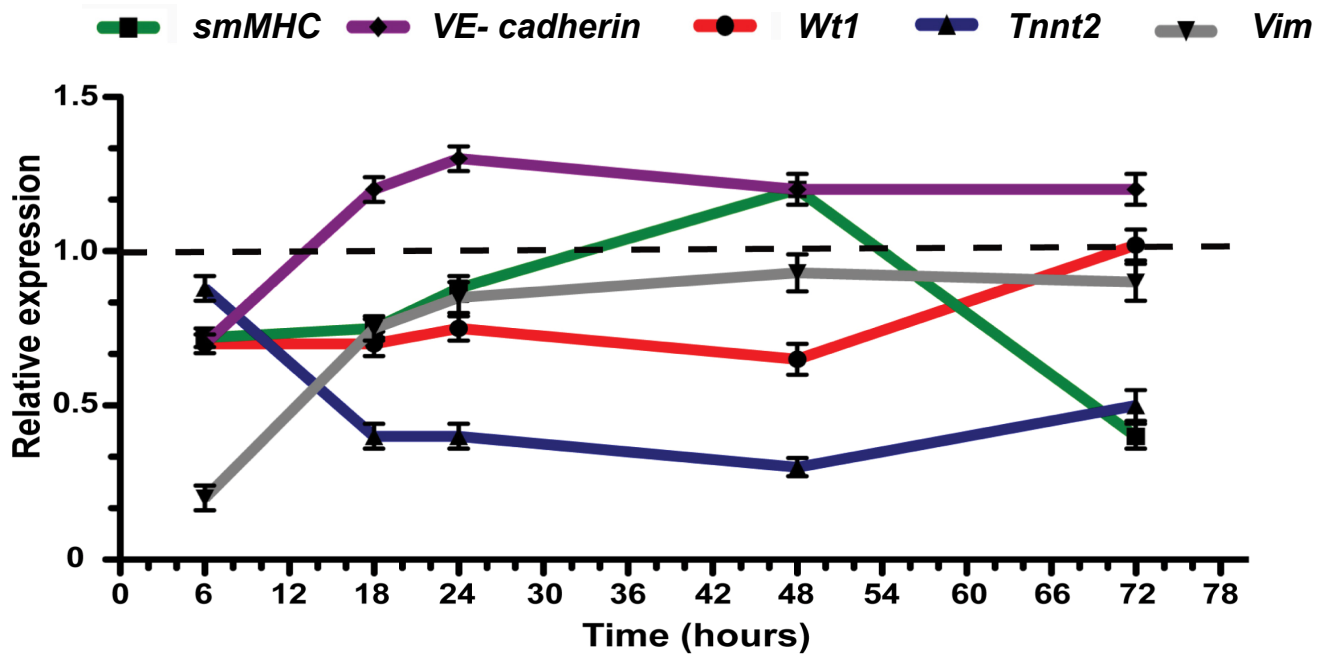
Suppl. Fig. 8. qRT-PCR, FACS analysis, and immunostaining demonstrating the effect of VEGF-A on epicardial cell fate in vitro.



WT1⁺ epicardial progenitors were isolated by FACS sorting dissociated Wt1^{GFP-Cre/+} hearts. Cells were cultured for 1 week in the presence or absence of VEGF-A. **a.** Gene expression measured using qRT-PCR, calculated relative to cardiac endothelial cells isolated from uninjured heart. **b.** Cell fate was determined by FACS. In the absence of VEGF-A (upper panel), cells largely retained WT1 expression and were predominantly vimentin⁺ or smMHC⁺. A lower fraction of cells expressed the endothelial markers PECAM1 or VE-Cadherin. In the presence of VEGF-A (lower panel), more cells upregulated KDR, PECAM1, or VE-Cadherin. **c.** Endothelial cell fate was also analyzed by immunostaining. WT1⁺ cells from adult Wt1^{GFP-Cre/+} heart were isolated by GFP FACS sorting and cultured for 1 week in the absence or presence of VEGF-A. VEGF-A upregulated VE-cadherin (white arrows), a specific marker for endothelial cells, in WT1⁺ cells. Bar= 5 μ m.

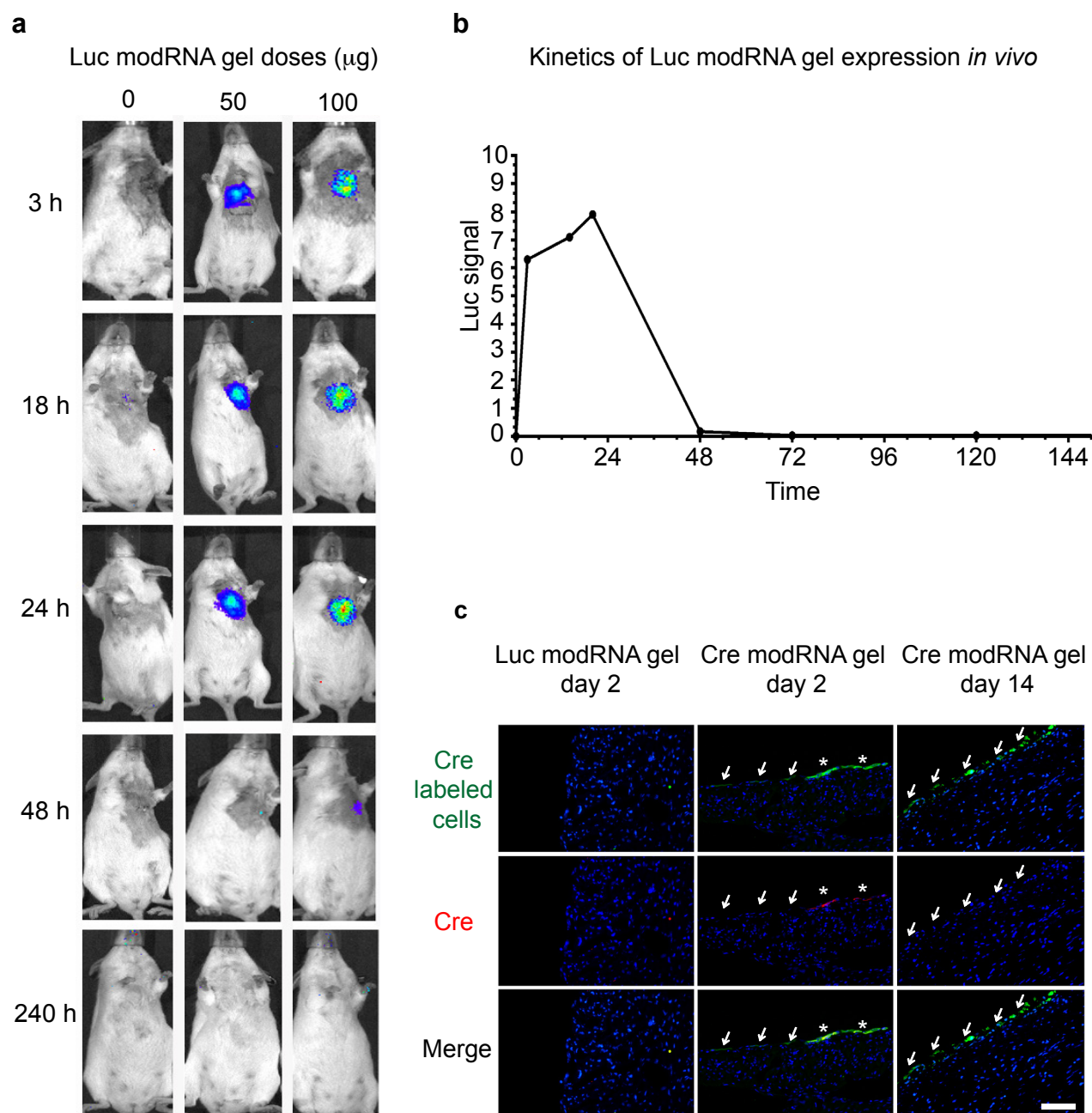


Suppl. Fig. 9 VEGF-A modRNA mobilized EPDCs (Wt1^{CreERT2} lineage) from the epicardial surface, enhanced their myocardial penetration, and stimulated differentiation into cardiovascular lineages. Hearts were analyzed 1 week after MI and VEGF-A modRNA or control treatment. EPDCs, labeled by Wt1^{CreERT2}, stay on the surface of the heart (white arrows) in the epicardial layer in the uninjured heart, or after MI and vehicle treatment. After MI and VEGF-A modRNA treatment, EPDCs entered the myocardium (c, white asterisks) and differentiated into endothelial cells (d, white asterisks). A small subset of EPDCs expressed the cardiomyocyte marker TNNI3 (d, yellow asterisks). Bar = 50 μ m.



Suppl. Fig. 10. The effect of VEGF-A on gene expression level in adult mouse cardiomyocytes, in vitro.

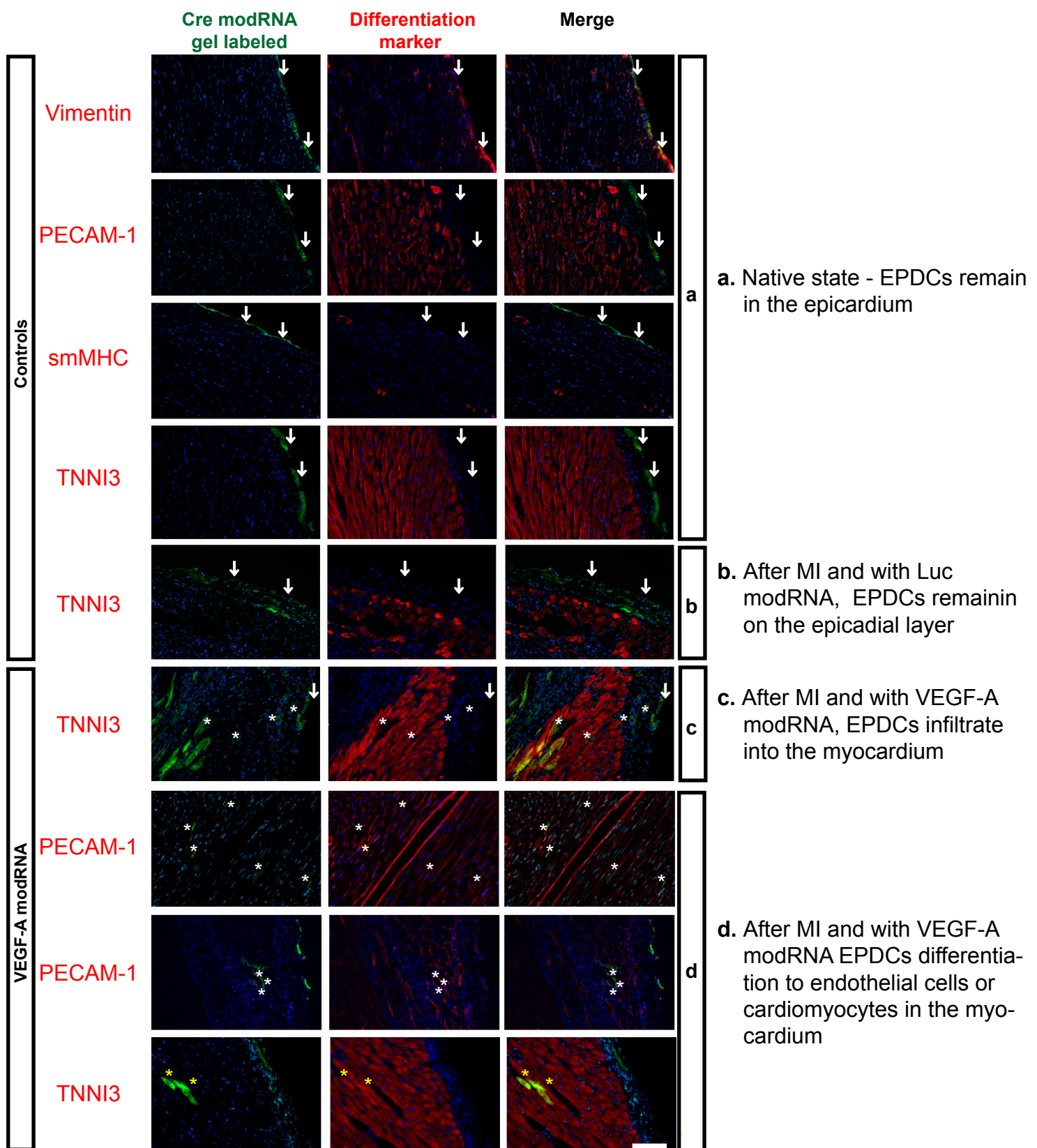
Gene expression level was evaluated for adult mouse cardiomyocytes at different time points post treatment with VEGF-A (5 μ g/ml). Adult mouse cardiomyocytes without VEGF-A treatments were used for normalization of expression levels (dashed line).



Suppl. Fig. 11. The kinetics of modRNA gel gene transfer to epicardial cells.

a-b. Indicated doses of Luciferase (Luc) modRNA gel were applied onto adult mouse hearts. Luciferase bioluminescence was measured at indicated time points.

c. Luc modRNA or Cre modRNA gel was applied onto adult Rosa26^{mTmG} mice hearts. 2 or 14 days later, hearts were fixed, cryosectioned, and immunostaining for Cre (red) or the Cre-activated GFP reporter (green). Images show Cre-activated GFP reporter cells with Cre expression (white asterisks) and without (white arrow). Bar = 50 μm .



Suppl. Fig. 12. VEGF-A modRNA mobilized EPDCs (labelled by Cre modRNA gel) from the epicardial surface and enhanced their myocardial penetration and differentiation into cardiovascular lineages. EPDCs were irreversibly labeled by “painting” the epicardial surface of R26^{mTmG} hearts with Cre modRNA gel, which activates GFP expression. 14 days later, hearts were treated with MI following intramyocardial injection of Luciferase (Luc, non-related modRNA) or VEGF-A modRNA. 7 days later, hearts were section and stain for GFP (green) and different markers (red). DAPI-stained nuclei are shown in blue. EPDCs stay on the surface of the heart (arrows) in the epicardial layer in uninjured hearts, or in MI hearts treated with Luciferase. However, after MI and injection of VEGF-A modRNA, EPDCs entered the myocardium (c. white asterisks) and differentiated into endothelial cells (d. white asterisks). A small subset of labelled cells expressed the cardiomyocyte marker TNNI3 (yellow asterisks). Bar = 50 μ m.